J|A|C|S
ARTICLES
Published on Web 05/07/2002

The Secret of Dimethyl Sulfoxide−Water Mixtures. A Quantum Chemical Study of 1DMSO−*n*Water Clusters

Barbara Kirchner*,† and Markus Reiher*,‡

Contribution from the Physikalisch-Chemisches Institut, Universität Zürich, Winterthurerstrasse 190, CH-8057 Zürich, Switzerland, and Theoretische Chemie, Universität Erlangen-Nürnberg, Egerlandstrasse 3, D-91058 Erlangen, Germany

Received December 7, 2001

Abstract: DMSO−water mixtures exhibit a marked freezing point depression, reaching close to 60 K at $n_{DMSO} = 0.33$. The phase diagram indicates that stable DMSO−water clusters may be responsible for this phenomenon. Using time-independent quantum chemical methods, we investigate possible candidates for stable supermolecules at mole fractions $n_{DMSO} = 0.25$ and 0.33. The model clusters are built by adding various numbers of water molecules to a single DMSO molecule. Structures and interaction energetics are discussed in the light of experimental and theoretical results from the literature. A comparison with results from molecular dynamics simulations is of particular interest. Our optimized structures are spatially very different from those previously identified through MD simulations. To identify the structural patterns characterizing the clusters, we classify them on the basis of hydrogen−acceptor interactions. These are well separated on an interaction energy scale. For the hydrophobic interactions of the methyl groups with water, attractive interactions of up to 8 kJ/mol are found. In forming clusters corresponding to a range of different mole fractions, up to four water molecules are added to each DMSO molecule. This corresponds to a rough local model of solvation. Examination of the trends in the interactions indicates that the methyl−water interaction becomes more important upon solvation. Finally, we investigate how the clusters interact and attempt to explain which role is played by the various structures and their intercluster interaction modes in the freezing behavior of DMSO−water.

1. Introduction

Many mixtures of water with organic solvents show properties deviating from ideality. For the system consisting of water and dimethyl sulfoxide (DMSO), extreme deviations from additivity are observed for a wide range of properties, such as density, viscosity, and adiabatic and isothermal compressibility.[1] At the mole fraction n_{DMSO} of ∼0.33, a very low freezing point (−140 °C) was measured.[2] The author suggested that a stable 1DMSO−2H_2O cluster could be responsible for this unusually low melting point. The phase diagram published afterward[3] is rather complex at the mole fractions $n_{DMSO} = 0.25-0.33$. In this case, the authors proposed the formation of a stable 1DMSO−3H_2O cluster.

Whereas the 1DMSO−2H_2O cluster has been seen many times in molecular dynamics (MD) simulation studies, no simulation[4−8] thus far has established the presence of a 1DMSO−3H_2O cluster, as no such structure was observed in the computer experiments. To solve the puzzle presented by this interesting mixture, we take one step back from MD simulations and focus on the interactions, i.e., the intermolecular potential. This is the heart of the MD simulation, as it determines the forces acting on all molecules and therefore the behavior of the system. It is also the point at which quantum chemistry and MD simulations meet.

Specifically, in this work, we examine closely the interaction energy of small DMSO−water clusters. A sequence of clusters is investigated, each consisting of one DMSO and up to four water molecules, corresponding, therefore, to a different mole fraction (see Table 1). For each cluster, lowest-energy structures are found and pair energies calculated.

The correspondence between cluster composition and mole fraction is made for three purposes: (i) to simplify the notation, (ii) to account for the fact that these clusters are observed to be the smallest entities in liquids,[4−8] and (iii) to understand whether the unusual behavior of a given mole fraction already appears at this level of abstraction.

In many ways, this system is a typical example of a dynamical ensemble, and it may at first glance appear counterintuitive to analyze it in terms of small static clusters. Our aim, however, is to try to understand why the MD simulations do not produce

* To whom correspondence should be addressed. E-mail: kirchner@unizh.ch. markus.reiher@chemie.uni-erlangen.de.
† Universität Zürich.
‡ Universität Erlangen-Nürnberg.

(1) Martin, D.; Hauthal, H. G. *Dimethylsulfoxid*; Akademie-Verlag: Berlin, 1971.
(2) Havemeyer, R. N. *J. Pharm. Sci.* **1966**, *55*, 851−853.
(3) Rasmussen, D. H.; MacKenzie, A. P. *Nature* **1968**, *220*, 1315−1317.
(4) Vaisman, I. I.; Berkowitz, M. L. *J. Am. Chem. Soc.* **1992**, *114*, 7889.
(5) Borin, I. A.; Skaf, M. S. *J. Chem. Phys.* **1999**, *110*, 6412−6420.
(6) Kirchner, B.; Searles, D. J.; Dyson, A. J.; Vogt, P. S.; Huber, H. *J. Am. Chem. Soc.* **2000**, *122*, 5379.
(7) Liu, H.; Müller-Plathe, F.; van Gunsteren, W. F. *J. Am. Chem. Soc.* **1995**, *117*, 4363.
(8) Luzar, A.; Chandler, D. *J. Chem. Phys.* **1993**, *98*, 8160.

10.1021/ja017703g CCC: $22.00

Table 1. Correspondence of Mole Fractions and Cluster Compositions

n_{DMSO}	No_{H_2O}	No_{DMSO}
0.5	1	1
0.33	2	1
0.25	3	1
0.2	4	1

a 1DMSO−3H_2O cluster and also why they are not able to explain the unusual behavior of the mixture at mole fraction $n_{DMSO} = 0.33-0.25$.

The article is organized as follows: The quantum chemical methodology used is described in detail in the next section. We then present the structures of the 1DMSO−$n$$H_2O$ clusters found to be minimums on the electronic potential energy surface (section 3) and classify the different types of hydrogen−acceptor interactions (section 4). The following section 5 gives a detailed evaluation of the interaction energetics in these clusters, including (section 5.2) an analysis of the contribution of the nuclei in addition to the purely electronic effects discussed so far. The assumption of pairwise additivity of these interactions is examined in section 6. Finally, section 7 gives a discussion of solvation effects.

2. Methodology

For this work, we used both density functional theory (DFT) and second-order Møller−Plesset (MP2) perturbation theory, to gain a consistent picture independent of quantum chemical method. The application of MP2 is particular important in this case, as the DFT results lack a correct description of dispersion interactions. For all quantum chemical structure optimizations, we used the density functional and ab initio programs provided by the TURBOMOLE 5.1 suite.[9] We employ the hybrid Hartree−Fock/DFT functional B3LYP[10,11] as implemented in TURBOMOLE. The B3LYP results were obtained from all-electron restricted Kohn−Sham calculations. For the MP2 calculations, we applied the resolution of identity (RI) technique.[12−16] The molecular orbitals, which are mainly of the character of 1s atomic orbitals of the DMSO sulfur atoms, are kept frozen in the MP2/RI calculations. Ahlrichs' TZVP basis set was used throughout, featuring a valence triple-ζ basis set with polarization functions on all atoms.[17] To analyze the electron density of the compounds, we made use of the concept of shared-electron numbers (SEN)[18] as implemented in TURBOMOLE. In this approach, interaction energies are evaluated semiquantitatively based on the shared electron numbers between a hydrogen atom and the corresponding acceptor atom. See ref 19 for details of this method. Partial charges were calculated according to Heinzmann and Ahlrichs[18] in Hilbert space and according to Cioslowski[20] on the basis of atomic polar tensors defined in real space.

All interaction energies (IE) were counterpoise-corrected using the procedure of Boys and Bernardi.[21,22] For the correction of the pair energy (IE_{pair}), two possibilities arise, namely

$$IE_{pair}(\phi_2) = \sum_i [E_{(AB)_i}(\phi_{2_i}) - E_{A_i}(\phi_{2_i}) - E_{B_i}(\phi_{2_i})] \quad (1)$$

and

$$IE_{pair}(\phi_{n+1}) = \sum_i [E_{(AB)_i}(\phi_{n+1}) - E_{A_i}(\phi_{n+1}) - E_{B_i}(\phi_{n+1})] \quad (2)$$

These formulations differ in the size of the basis sets used for the calculation of dimer and monomer energies. While ϕ_{2_i} denotes all basis functions of the molecule pair i constituting a dimer, ϕ_{n+1} is the full basis of the entire 1DMSO−$n$$H_2O$ cluster. Obviously, ϕ_2 equals ϕ_{n+1} in case of the 1DMSO−1H_2O configurations. For neon trimers, it has been shown that the difference between the two possibilities is negligible.[23] We therefore chose the latter way of calculating interaction energies for practical reasons. Note that the definition of the total and pair interaction energies excludes the energy contribution from the conformational relaxation of the fragments when the complex is being formed. This is in line with current definitions of complex interaction energy (ref 24, p 1377) (structural relaxation would change the interaction energies only by ~1 kJ/mol per molecule in the supermolecule).

Whereas the counterpoise correction has been applied to all interaction energies, it has not been applied during the optimization procedure. Test optimizations with larger basis sets confirmed negligible deviations to our minimum structures.

To visualize a potential electron-pair interaction, we utilized the electron localization function (ELF). ELF is a measure for the spherically averaged Fermi hole around a reference electron. As described by Becke and Edgecombe,[25] the function can be mapped onto an interval $0 < ELF < 1$. $ELF \approx 1$ indicates areas of a localized exchange potential. Such areas are occupied by electron pairs. All ELF plots were generated with the Car-Parrinello MD package of the Parrinello group.[26]

For the vibrational analysis, the second derivatives of the total electronic energy were computed as numerical first derivatives[27,28] of the analytic energy gradients obtained from TURBOMOLE. The vibrational frequencies and the zero-point vibrational energies were obtained within the harmonic approximation. For the calculation of the ΔD_0 values, the zero-point energy differences were added to the total electronic energy differences.

The program MOLDEN[29] was used to visualize the structures.

3. Structures of DMSO−Water Clusters

In this section, the structures from B3LYP optimizations are presented, leaving the discussion on the energetics for section 5. We consider the DMSO−H_2O clusters as supermolecules,

(9) Ahlrichs, R.; Bär, M.; Häser, M.; Horn, H.; Kölmel, C. *Chem. Phys. Lett.* **1989**, *162*, 165−169.
(10) Becke, A. D. *J. Chem. Phys.* **1993**, *98*, 5648−5652.
(11) Stephens, P. J.; Devlin, F. J.; Chabalowski, C. F.; Frisch, M. J. *J. Phys. Chem.* **1994**, *98*, 11623−11627.
(12) Haase, F.; Ahlrichs, R. *J. Comput. Chem.* **1993**, *14*, 907.
(13) Eichkorn, K.; Treutler, O.; Öhm, H.; Häser, M.; Ahlrichs, R. *Chem. Phys. Lett.* **1995**, *240*, 283−290.
(14) Eichkorn, K.; Weigend, F.; Treutler, O.; Ahlrichs, R. *Theor. Chem. Acc.* **1997**, *97*, 119−124.
(15) Weigend, F.; Häser, M. *Theor. Chem. Acc.* **1997**, *97*, 331−340.
(16) Weigend, F.; Häser, M.; Patzelt, H.; Ahlrichs, R. *Chem. Phys. Lett.* **1998**, *294*, 143.
(17) Schäfer, A.; Huber, C.; Ahlrichs, R. *J. Chem. Phys.* **1994**, *100*, 5829−5835.
(18) Heinzmann, R.; Ahlrichs, R. *Theor. Chim. Acta* **1976**, *42*, 33−45.
(19) Reiher, M.; Sellmann, D.; Hess, B. A. *Theor. Chem. Acc.* **2001**, *106*, 379−392.
(20) Cioslowski, J. *J. Am. Chem. Soc.* **1989**, *111*, 8333−8336.
(21) Boys, S. F.; Bernardi, F. *Mol. Phys.* **1970**, *19*, 553−566.
(22) van Duijneveldt, F. B.; van Duijenveldt-van de Rijdt, J. G. C. M.; van Lenthe, J. H. *Chem. Rev.* **1994**, *94*, 1873.
(23) Ermakova, E.; Solca, J.; Steinebrunner, G.; Huber, H. *Chem. Eur. J.* **1998**, *4*, 373−382.
(24) Jeziorski, B.; Szalewicz, K. Intermolecular Interactions by Perturbation Theory. In *Encyclopedia of Computational Chemistry*; Schleyer, P. v. R., Ed.; J. Wiley & Sons: Chichester, U.K., 1998; pp 1376−1398.
(25) Becke, A. D.; Edgecombe, K. E. *J. Chem. Phys.* **1990**, *92*, 5397−5403.
(26) Hutter, J.; et al. CPMD. IBM Research Division, Zürich Research Lab. MPI für Festkörperforschung, Stuttgart 1995−1999. MPI FKF Stuttgart/Zürich, 1995.
(27) Kind, C.; Reiher, M.; Neugebauer, J.; Hess, B. A. SNF, University of Erlangen-Nürnberg, 2001.
(28) Hess, B. A. NUMFREQ, University of Erlangen-Nürnberg, (based on work by Grimme, S.; Marian, C.; Gastreich, M.; 1998, University of Bonn) 2001.
(29) Schaftenaar, G.; Noordik, J. H. *J. Comput.-Aided Mol. Des.* **2000**, *14*, 123−134.

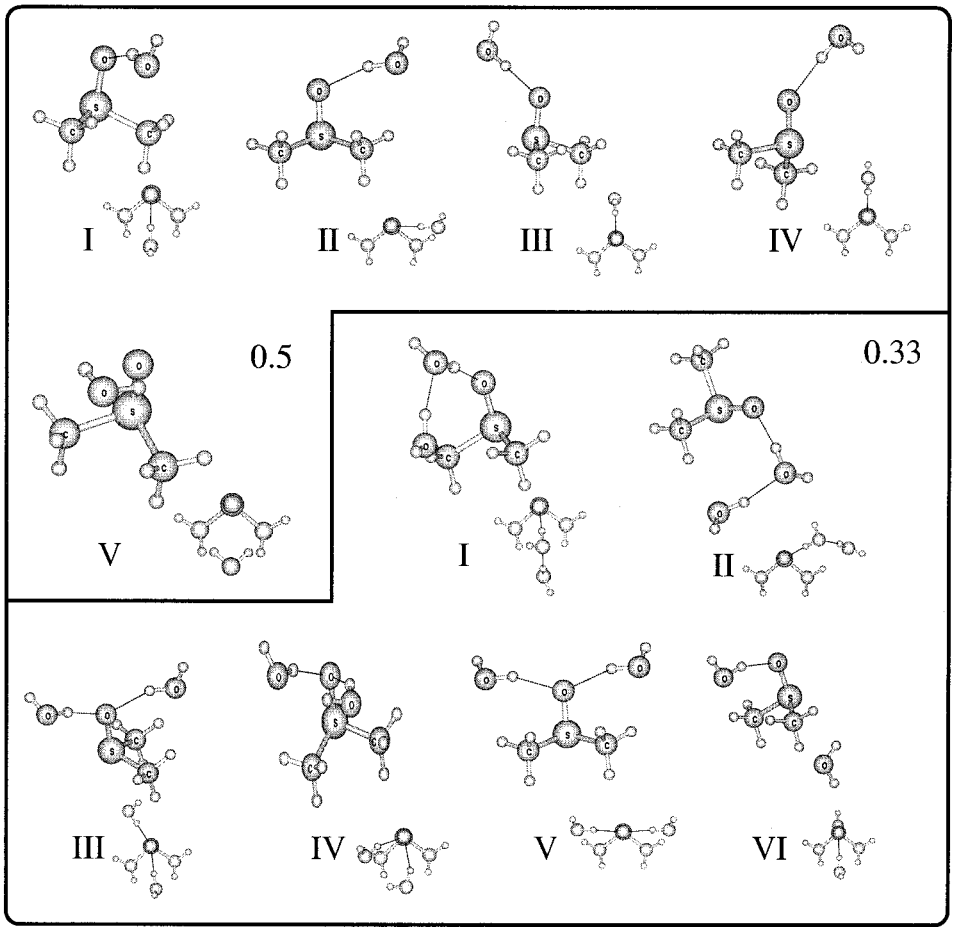

Figure 1. Configurations of the smaller clusters. An additional view from the top of the cluster has been added for clarity. All structures are fully optimized minimums on the potential energy surface, except structure 0.5-V, which was optimized in C_s symmetry and turned out to be a first-order saddle point. The structures depicted were obtained from B3LYP calculations. The MP2/RI structures are very similar and could not be distinguished from the B3LYP structures in these representations.

treating the component molecules as units without ingoring the intramolecular energetics. We refer to a particular structure at a given mole fraction as a *configuration*.

Figure 1 and Figure 2 depict all optimized minimum-energy configurations at the different mole fractions.

As it is also part of this study to test how well the assumption of pairwise additivity works,[1] we started the optimizations not only from configurations that looked like possible candidates for the global minimum but also from some unfavorable-looking structures. (Pairwise additivity is a general approximation in MD simulations. It means that all interactions between pairs of atoms are summed up to give the total interaction instead of treating the system as a whole. In principle, many-body effects are neglected (see also standard textbooks[30]). Our reasoning was that many-body effects do not only occur at global minimum structures. For instance, one study proposed a cluster in which the oxygen atom of a water molecule is quite close to the DMSO sulfur atom.[31] Although seeming nonintuitive at first glance, upon closer examination, this starting structure seems favorable, because of the partial charges on the S and O atoms: $Me_2S^{\delta+} = O^{\delta-}$. However, after relaxation, we unexpec tedly obtained configuration VI for $n_{DMSO} = 0.33$, dubbed 0.33-VI, in which the oxygen atom of the water molecule is further away from the sulfur atom than its hydrogen atoms (compare Figure 1).

We refer to configurations 0.5-I, 0.33-I, 0.25-II, and 0.2-I as 'Rüssel' configurations (from the German: Rüssel = trunk) because all water molecules are arranged in a trunklike manner.

Examining the overall structural features, we find that the S−O distance is only slightly enlarged upon H_2O coordination. Adding one water molecule increases the double-bond distance by ∼2 pm (1 pm) with B3LYP (MP2/RI), and with two water molecules, this increases to ∼3 pm (2 pm). Thus, the nature of the S−O double bond is hardly affected by water coordination. The Me−S−Me angle changes by less than 1.5° (with B3LYP and also with MP2/RI) upon coordination of water molecules.

Comparing the two methods used, we find that the B3LYP and MP2/RI structures agree very well. The intramolecular distances in DMSO and H_2O differ generally only by ∼0.5 pm and the angles by ∼1°. Occasionally, bond length deviations of up to 2.5 pm are observed. As one would expect, the intermolecular distances, i.e., the hydrogen bond distances, seem to be less well described by B3LYP. Here, we find deviations from MP2/RI by up to 10 pm. But note that most hydrogen bond distances calculated with the two methods differ by less than ∼3 pm. The global structure of a cluster after optimization is essentially the same for B3LYP and MP2/RI.

(30) Allen, M. P.; Tildesley, D. J. *Computer Simulations of Liquids*; Oxford, 1987.
(31) Thommilla, E.; Murto, M. *A. Chem. Scand.* **1963**, *17*, 1947−1956.

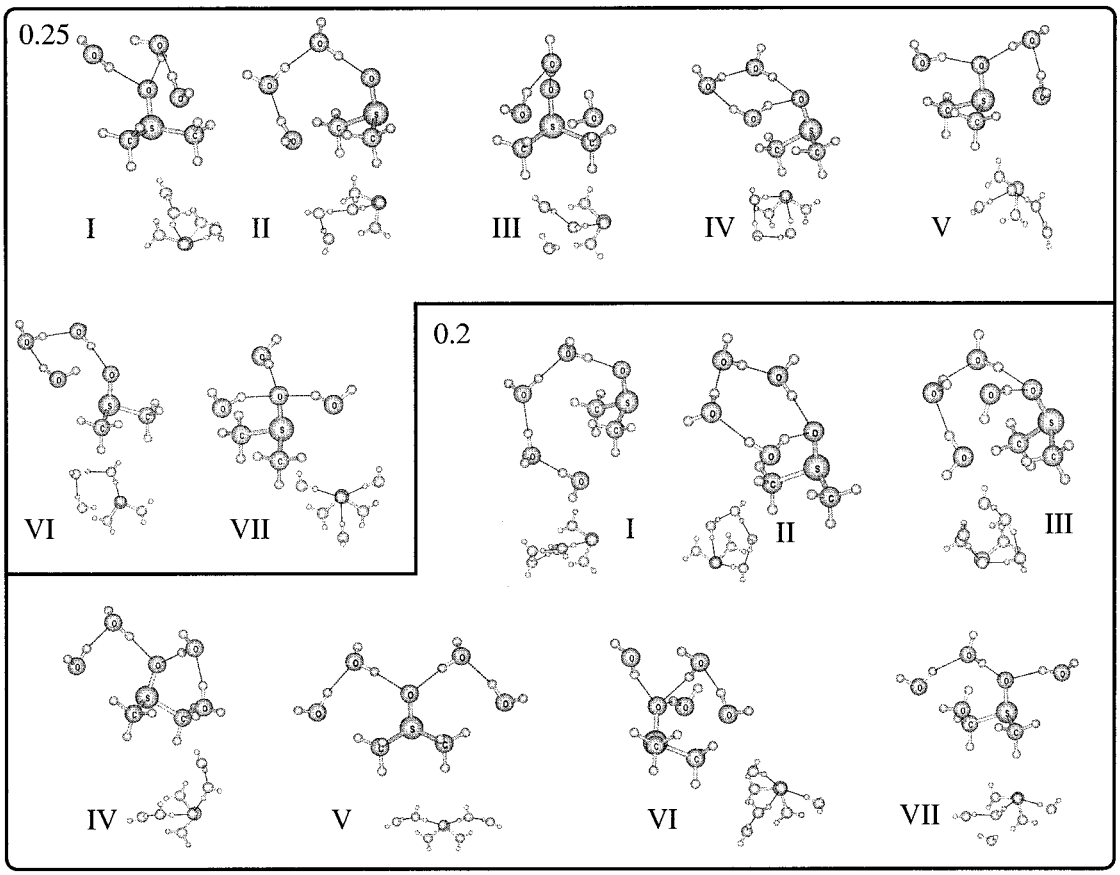

Figure 2. Configurations of the larger clusters with additional view from the top. The structures depicted were obtained from B3LYP calculations. The MP2/RI structures are very similar and could not be distinguished from the B3LYP structures in these representations.

4. Classification of Hydrogen−Acceptor Interactions as a Key Structural Feature of Different Configurations

In view of the variety of different configurations occurring at each mole fraction (Figures 1 and 2), the need to identify the key structural characteristics of each arises. Elements characterizing the differences between the configurations are given by dividing the different intermolecular bonds into categories. The following four types of intermolecular-bonding modes, which are well separated according to their different interaction energies, may be distinguished (Note that the structural parameters correspond to the particular interaction energy given; deviations from these distances and angles would also change the interaction energy, although its character is maintained within a certain interval. Furthermore, we aim at method-independent interaction energies and give only the particular method in those cases where significant deviations between B3LYP and MP2/RI occur.):

4.1. DMSO−Oxygen−Water−Hydrogen Bonds (Type H1). The strongest interactions are found between the DMSO−oxygen atom and a water−hydrogen atom. These interactions are as strong as ∼30 kJ/mol, which can be extracted from the interaction energy of a water and a DMSO molecule in structure 0.5-III (see also Table 4), where the H···O distance is 186.5 pm at an O···O−H angle of 2.1°. (The angle is measured from the acceptor oxygen atom to the donor oxygen atom to the hydrogen atom itself.)

We briefly note that we find the hydrogen bond of water−DMSO to be more stable than the hydrogen bond of the water dimer, in agreement with refs 32 and 33. The increased hydrogen bond energy may be understood in terms of electrostatic attraction. We calculated partial charges obtained from two different population analyses, namely, the one by Ahlrichs and co-workers and the one by Cioslowski (for details on these methods see section 2). We used both analyses since the partial charge of an atom is not a well-defined quantum mechanical quantity and is thus affected by a certain arbitrariness. In this case, both population analyses show a clear distinction between the partial charges of oxygen atoms in water and DMSO. The partial charge is ∼−0.7 for DMSO oxygen atoms and −0.4 for water oxygen atoms (using Ahlrichs' population analysis). The strong DMSO−water hydrogen bond can therefore be attributed to an increased electrostatic contribution due to the more strongly polarized oxygen atom in DMSO.

4.2. Intermolecular Water−Oxygen−Water−Hydrogen Bonds (Type H2). (i) Relaxed Hydrogen Bonds (Type H2a). When two water molecules interact via one hydrogen and one oxygen atom, an optimum structure for the hydrogen bond results. These intermolecular bonds possess interaction energies of ∼20 kJ/mol at a distance of ∼197 pm and an optimal ···O−H angle of almost 0° (compare with the highly accurate water dimer energies (20.5−22.6 kJ/mol) published in ref 24 and references therein).

(ii) Strained Hydrogen Bonds (Type H2b). Occasionally, all three atoms of a water molecule are involved in the hydrogen

(32) Zheng, Y.; Ornstein, R. L. *J. Am. Chem. Soc.* **1996**, *118*, 4175−4180.
(33) Luzar, A.; Soper, A. K.; Chandler, D. *J. Chem. Phys.* **1993**, *99*, 6836−6847.

Table 2. B3LYP/TZVP Interaction Energies Obtained with the SEN Method (in kJ/mol)[a]

configuration	pair	σ_{HA}	IE $_{SEN}$	r_{B3LYP}	$r_{MP2/RI}$
0.33-IV	H(W1)···O(D)	0.0545	−28.0	186.4	182.5
	O(W1)···H1(D)	<0.0050	<−2.6	321.5	310.3
	O(W1)···H1b(D)	<0.0050	<−2.6	301.9	296.3
	H(W2)···O(D)	0.0322	−16.6	204.7	201.6
	O(W2)···H2(D)	<0.0050	<−2.6	267.8	251.3
	O(W2)···H1(D)	<0.0050	<−2.6	261.6	255.8
	H(W2)···O(W1)	0.0138	−7.1	227.7	235.7
0.33-II	H(W1)···O(D)	0.0704	−36.2	176.1	174.1
	H(W2)···O(W1)	0.0634	−32.6	180.4	179.1
	O(W2)···H(D)	0.0148	−7.6	222.3	222.6

[a] Only an upper bound is given for SENs less than the threshold of 0.005. Water molecules are abbreviated as W and DMSO as D. Donor−acceptor distances are given for B3LYP and MP2/RI (in pm).

bond network, because rings involving only the hydrogen−acceptor oxygen atom of DMSO lack a hydrogen donor atom from DMSO. (see also section 5). In this case, the optimum distance and angle of H2a cannot be achieved. This intermolecular bond energy cannot be estimated from the decomposition of a cluster; i.e, it is not possible to attribute the decomposition energy solely to the broken hydrogen bond. An alternative way to obtain the energy of this bond is given by the SEN method[19] (see Table 2 and section 2 for details on the method). We chose configuration 0.33-IV with a total B3LYP interaction energy of −67.8 kJ/mol (cf. Table 4) and distributed this energy between the three different contacts of the water molecule under consideration. The hydrogen bond energy for the strained H···O bond with H−O distance 225 pm and O···O−H angle 35.2° is less than 10 kJ/mol.

Note that strained hydrogen bonds also occur in those configurations where attraction by the methyl groups of DMSO are important, as in the case of 0.25-IV.

4.3. Water−Oxygen−Methyl−Hydrogen Contacts (Type H3). As we observed many configurations featuring the oxygen atom of a water molecule in close proximity to a hydrogen atom of the DMSO methyl group, we were curious to see whether there is a pronounced attraction between the two. We call this interaction a *contact*, because its interaction energy may range from very weak to strong intermolecular bonding. Table 2 gives estimates for the H3-type contacts in 0.33-IV and 0.33-II calculated by the SEN method. Indeed, it is found that the energy of the H3 contacts in 0.33-IV, in which the water−oxygen−methyl−hydrogen distance is larger than 261.6 pm at an O···C−H angle of 32.6°, is less than 2.6 kJ/mol (for B3LYP). However, it is ∼8 kJ/mol in 0.33-II for the 223.0 pm contact at an O···C−H angle of 9.7°. Although the H3-type contacts are rather weak in comparison to the others we have described, these interactions are found to be decisive for the global minimum structures.

For a qualitative understanding of attractive and repulsive interactions in DMSO−water clusters, it is instructive to examine the ELF. Values close to unity indicate a high probability for finding a pair of electrons in a given spatial region.

The ELF isosurface for the 1DMSO−1H_2O optimized structure, which is depicted in Figure 3, demonstrates that the DMSO−oxygen lone pairs appear as a doughnut-shaped ring, indicating that this oxygen atom does not exhibit strong preferential coordination by itself. ("Preferential corrdination"

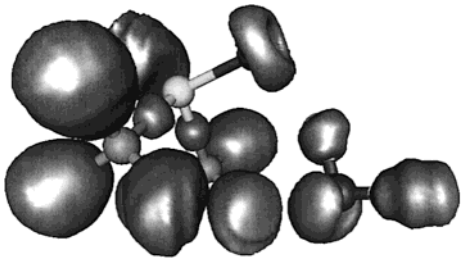

Figure 3. ELF isosurface (ELF = 0.85) for the lowest-energy structure of 1DMSO−1H_2O. The lone pair at the sulfur atom, the doughnut-shape lone pairs at the DMSO oxygen atom, and the lone pairs at the H_2O oxygen atom are visualized. Note the interaction of the water oxygen lone pairs with the methyl group hydrogen atoms, resulting in a reduced probability of finding a localized electron pair in between.

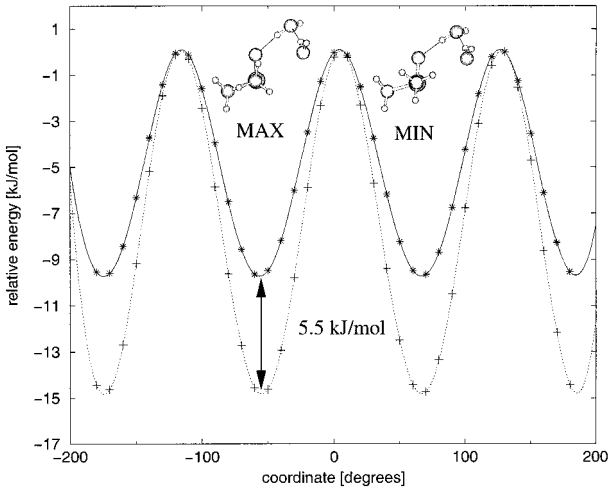

Figure 4. Rotation curve of a methyl group in 0.33-II (pluses, calculated points; dotted line, spline) and in DMSO alone (stars, calculated points; solid line, spline) calculated with B3LYP/TZVP.

shall denote the situation where certain coordination positions along the ring around the DMSO oxygen atom are favored over others.) This is in agreement with previous MD simulations. However, in this structure, the water molecule is clamped in place by the methyl groups, whose interaction with the water oxygen atom is expressed by the deformed ELF isosurface of the participating C−H moiety. We thus note that preferential coordination to the DMSO oxygen atom exists because of these "secondary" interactions with the methyl groups.

To examine the important role played by the methyl groups in an alternative way, we calculated the rotation curve of a methyl group in configuration 0.33-II. We chose this configuration because it provides one short methyl group contact. Since we must also consider contributions coming from the other methyl group or the DMSO oxygen atom, we additionally calculated the rotation of a methyl group in an isolated DMSO molecule.

In Figure 4, both rotation curves are shown. The maximum and the minimum structures are also depicted. The configuration where the methyl group is staggered with the S−O axis is the structure of maximum energy (i.e., least preferred). Each extremum of this smooth rotation curve corresponds to one hydrogen atom of the methyl group coming from an unpreferred position, rotating to a favorable position, and leaving it again. The difference in energy between minimum and maximum positions comes to 15 kJ/mol.

Table 3. Order of Stable Configurations for Different Mole Fractions[a]

		structural features		B3LYP	MP2/RI	B3LYP
n_{DMSO}	no.	rings	H1 H2a H2b H3	ΔIE	ΔIE	ΔD_0
0.5	I	2 × 6	1 0 0 2	0.0	0.0	0.0
	II	1 × 6	1 0 0 1	6.1	5.2	5.5
	III		1 0 0 0	10.4	9.4	8.6
	IV		1 0 0 0	15.0	13.7	13.5
	V		0 0 0 0	19.6	16.5	16.6
0.33	I	2 × 8	1 1 0 2	0.0	0.0	0.0
	II	1 × 8	1 1 0 1	7.2	6.7	6.8
	III	2 × 6	2 0 0 2	16.2	12.8	13.4
	IV	3 × 6	2 0 1 2	16.5	11.5	16.3
	V	2 × 6	2 0 0 2	17.2	13.1	15.4
	VI	2 × 6	1 0 0 2	32.3	25.3	27.4
0.25	I	2 × 8 2 × 6	2 1 1 2	0.0	0.0	0.0
	II	2 × 10	1 2 0 3	0.1	1.4	−1.4
	III	2 × 8 1 × 6	1 1 2 2	1.8	2.1	2.3
	IV	1 × 8 2 × 6	2 1 1 2	2.3	1.9	3.1
	V	1 × 8 2 × 6	2 1 0 2	3.6	2.6	1.4
	VI	1 × 8 1 × 6	2 1 1 1	8.9	8.9	8.7
	VII	4 × 6	3 0 0 3	18.2	13.3	16.5
0.2	I	2 × 12	1 3 0 3	0.0	0.0	0.0
	II	1 × 10 2 × 6	2 2 1 2	4.7	6.2	5.6
	III	3 × 10	2 2 0 3	5.2	4.7	9.6
	IV	3 × 8	2 2 0 3	5.3	4.5	4.4
	V	2 × 8	2 2 0 2	14.4	13.8	12.8
	VI	2 × 8 2 × 6	3 1 0 3	16.7	12.9	15.6
	VII	2 × 8 2 × 6	2 1 0 4	18.7	14.5	26.5

[a] The interaction energies ΔIE are given relative to the minimum configuration of the particular mole fraction obtained with B3LYP and MP2/RI calculations. The last column gives the B3LYP interaction energies corrected for the zero-point vibrational energy, ΔD_0. The third to sixth columns contain characteristic structural features of the particular configurations. All energies in kJ/mol.

The rotation of a methyl group in DMSO yields a rotation curve profile with 9.5 kJ/mol amplitude (Figure 4). This is ∼3 kJ/mol more than calculated in ref 37. Subtracting this contribution from the total above leaves an energy for the attractive methyl group contact of 5.5 kJ/mol. On building the hydrogen contact, the C−H distance of the methyl group hydrogen atom, which is closest to the oxygen atom of the water molecule, is elongated very little (by at most 0.4 pm). This is expected, as the strong covalent C−H bond is disturbed only by the weak intermolecular attraction of the water oxygen atom. These effects are so small that a detailed analysis of C−H bond length changes, charge, and energy transfers in the hydrogen-bonded complex would not lead to useful results, keeping in mind that most charge or energy decomposition analyses are not well defined from the viewpoint of fundamental quantum mechanics.

5. Energetics of the optimized structures

5.1. Results and Discussion. To determine the lowest-energy structure of our configurations, we calculated the interaction energy for each of them. The basis set superposition error is of the order of 5 kJ/mol per interacting pair of molecules and must not be neglected. Therefore, all interaction energies are fully counterpoise-corrected. Table 3 lists the relative interaction energies of all configurations.

To characterize the structures alternatively to the classification in section 4, we give in the third column the number of ring structures present in the particular configuration. For example "1 × 6" means one ring consisting of six atoms. Most of the rings include four atoms from the DMSO molecule but sometimes only the oxygen atom. If other atoms of DMSO are involved, there is always one large methyl−hydrogen−water−oxygen separation distance. If this distance is larger than 290 pm, the structure is not counted as a ring. In addition, the number of different types of intermolecular interactions as classified in the previous section is given for each configuration. In the next three columns, the difference between the interaction energy of the lowest-energy configuration and the configuration considered in a particular row is given. The energies are listed for B3LYP, MP2/RI, and B3LYP corrected for zero-point vibrational energy.

Within the configurations considered, the lowest-energy structures at mole fractions $n_{DMSO} = 0.5$, 0.33, and 0.2 are our global minimum structures as the next lowest structures are approximately 5−7 kJ/mol higher in energy. This is larger than the error of the methods we used, which we expect to be less than 5 kJ/mol. For mole fraction $n_{DMSO} = 0.25$, the identification of the lowest-energy configuration is impossible since all structures are energetically too close to be clearly distinguishable, although they are spatially very different. In addition, we found that the average number of unsaturated contacts, i.e., contacts that have not been used for intracluster bonds, is low at this particular mole fraction. The energetics at mole fraction $n_{DMSO} = 0.2$ seem to be already dominated by the pure water hydrogen bond network. At every mole fraction, there exist configurations in which an additional methyl group contact leads to more stable configurations. (Compare for example 0.5-II and 0.5-I, 0.33-II and 0.33-I, 0.25-VI and 0.25-IV, and 0.2-V and 0.2-IV).

By closer inspection, rules of thumb can be given, which are complementary to the classification of hydrogen−acceptor interactions in section 4. These can make it possible to predict how minimum structures of clusters that have not yet been studied may look, similar to the rules for hydrogen bonding in pure water:[34] Ring structures are more favorable than no-ring structures (compare 0.5-III (no ring) versus 0.5-II (one ring) or 0.33-II (one ring) with 0.33-I (two rings)). This is reflected in the fact that more H3 contacts lead to a more stable configuration. Only rings of even numbers are possible as a donor has to be followed by an acceptor and so on. This is the reason disadvantageous features in configurations appear; i.e., all atoms of a water contribute to a ring, if the DMSO oxygen atom is taking part and a donor hydrogen atom is missing. Such features are observed, e.g., in configurations 0.5-V, 0.33-IV, 0.25-IV, and 0.2-III. Rings that include eight atoms are more favorable than rings which that only six atoms. (Compare configuration 0.33-I (two eight-rings) versus 0.33-V (two six-rings) or 0.25-II (two eight-rings and one six-ring) and 0.25-V (one eight-ring and two six-rings)). It is most likely, but not certain, that large rings are less favored. Comparing 0.25-I and 0.25-II, the configuration with the larger rings is not favored, but in 0.2-I versus 0.2-III, the large ring configuration is the lowest-energy structure.

Comparing the two methods, MP2/RI and B3LYP, we find that the lowest-energy configurations are identical. The discus-

(34) Ludwig, R. *Angew. Chem., Int Ed.* **2001**, *40*, 1808−1827.
(35) Carles, S.; Desfrançois, C.; Schermann, J. P.; Bergès, J.; Houèe-Levin, C. *Int. J. Mass Spectrom.* **2001**, *205* 227−232.
(36) Vishnyakov, A.; Lyubartsev, A. P.; Laaksonen, A. *J. Phys. Chem. A* **2001**, *105*, 1702−1710.
(37) Mezey, P. G.; Kapur, A. *Can. J. Chem.* **1980**, *58*, 559−566.

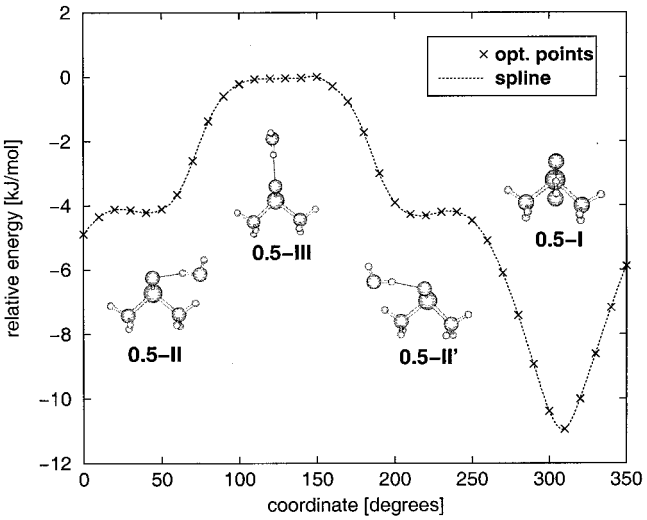

Figure 5. Rotation curve to distinguish between configurations of [35] and of [32]. The water molecule rotates along the DMSO sulfur−oxygen axis under partial relaxation (B3LYP/TZVP).

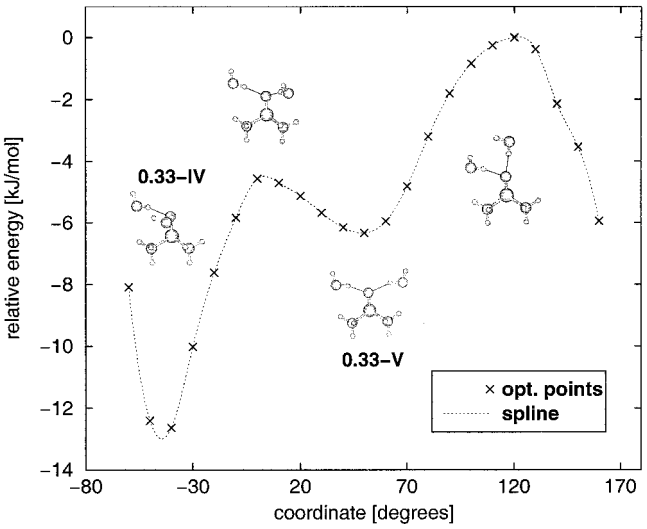

Figure 6. Rotation curve calculated with B3LYP/TZVP in order to investigate preferential coordination. One water molecule is kept fixed, while the second rotates along the DMSO sulfur−oxygen axis under partial relaxation.

sion so far applies also for MP2/RI. The only differences are that configuration 0.33-III is higher in energy than configuration 0.33-IV and 0.25-III is higher in energy than 0.25-IV, but these differences lie within the range of error of the methods.

5.2. Contributions from the Nuclei. So far, we have discussed the purely electronic effects on the stabilization of different DMSO−H_2O clusters. Since the potential energy wells of the total electronic energy may be shallow for weak hydrogen−acceptor interactions, we should investigate the effect of the nuclei at 0 K and at standard temperature. Values for ΔD_0 for all configurations are given in Table 3. The energetic order of configurations given in Table 3 is unchanged. However, there are two exceptions of minor importance. First there is the Rüssel structure 0.25-II, which is electronically a little more unstable than the lowest-energy structure, 0.25-I. The zero-point energy correction favors this Rüssel structure by 1.4 kJ/mol. Configuration 0.2-III is much less stable when accounting for zero-point effects, which changes the order of structures 0.2-II, 0.2-III, and 0.2-IV (compare Table 3). However, these changes are within the range of uncertainty of the quantum chemical methods we used. The results for the corresponding enthalpies at standard temperature are similar. Since we only discuss significant differences between different configurations, we need not take into account the contributions from the vibrations of the nuclei. In conclusion, we find that the structural peculiarities of the configurations are of an electronic nature and hardly affected by contributions from the nuclei. It should be noted that these conclusions are drawn on the basis of vibrational frequencies obtained from a quantum chemical *harmonic* force field. With respect to this, our model for the description of effects from the nuclei, particularly for their entropic contributions, is rather limited and further investigations are necessary.

5.3. Comparison with the Literature. While our results are in accordance with ref 35 at mole fraction $n_{DMSO} = 0.5$, we cannot confirm the results of ref 32. To be certain that we indeed obtained the global minimum, we calculated the rotation curve of one water molecule about the DMSO oxygen−sulfur axis. This rotation curve is displayed in Figure 5.

Whereas configuration 0.5-II and the configuration closest to that proposed in ref 32 are local minimums of this rotation curve, configuration 0.5-I is indeed the global minimum. By looking at the sequence of this rotation, 0.5-III, 0.5-II, and 0.5-I, it can be realized that in each step a methyl group contact is gained. Looking now closely at the energy, the first methyl contact leads to a gain in energy of 4.3 kJ/mol, whereas the next step yields another 6.3 kJ/mol. From a sterical point of view, one would expect exactly the opposite. The water molecule looks as if it would be exposed to so much tension that one would anticipate a decreasing energy for the second methyl group contact. However, the difference between both angles in the minimum configuration and the angle of the 0.5-II is ∼5° more favorable for the minimum structure. This is also in accordance with, and maybe due to, the fact that the second hydrogen bond yields more energy for the same water molecule than the first.[34]

Our lowest-energy configuration at mole fraction $n_{DMSO} = 0.33$ does not match the findings of MD simulation work. Almost all simulation studies observe configurations similar to 0.33-IV or 0.33-V at this concentration. In ref 36, the way in which two water molecules might be distributed around the DMSO oxygen atom is discussed: "If the two water molecules are in the first solvation shell, they are located on opposite sides of the ring. Interestingly, there are no preferential orientations of these two waters relative to DMSO methyl groups." As we did find in our results preferential coordination of the two water molecules, we support our findings by another rotation curve of one water molecule about the DMSO oxygen−sulfur axis, where a second water molecule was kept fixed, shown in Figure 6.

Undoubtedly, we also located the global minimum in this case. We find strong preferential coordination. In section 4, we attributed the particular positions for the addition of water molecules to secondary effects of the methyl groups, even though the DMSO oxygen atom exhibits coordination sites where both water ligands could come from any direction in space, i.e., where all coordination positions along the ring around the DMSO oxygen atom are available.

Only once a brief appearance of a 1DMSO−$3H_2O$ cluster is mentioned in MD simulation work.[4] The configuration described

looks like our configuration 0.25-VIII, but because of its short appearance, it was not considered to be stable by the authors. As in ref 36, a stable 1DMSO−3H_2O configuration also failed to appear, the authors used a very sophisticated spatial distribution function to predict the structure of this cluster. The authors propose that if two water molecules are already donating protons to the oxygen in the S═O group, there would be a possibility for a third water molecule from the second hydration shell to form hydrogen bonds to the first two water molecules, similar to configuration 0.25-IV or 0.25-VI.

While there has been no consensus among the MD simulation work on whether the methyl groups could be involved in the interaction with water, our work points toward minimum configurations where a water molecule does interact with the methyl groups. In ref 36, no preferential coordination of two water molecules to one DMSO molecule is found. Nevertheless it is admitted that the united-atom ansatz could blur this interaction with the methyl groups.

In ref 4, the radial pair distribution function is given, which provides knowledge about the structure of a liquid. The peak of the water−oxygen−DMSO−carbon function is found at shorter distance than that of the water−hydrogen−DMSO−carbon function; i.e., on average, the MD simulations show the methyl groups closer to the oxygen atoms of the water molecules than to the hydrogen atoms. Luzar et al.[33] criticized the authors of ref 4 for interpreting their results as indicating the presence of a weak O-methyl group hydrogen bond. Luzar et al. attributed their own observations and those of Vaisman and co-workers to packing effects.

6. Pairwise Additivity

In the previous section, we identified the minimum configurations for each cluster. We found the structures to deviate from those discussed in MD simulation work; therefore, we test in this section the extent to which the pairwise additivity assumption is valid. We calculated for every cluster all energies given by the different possible pairs of molecules in exactly the same geometrical arrangement as in the cluster and added them up to give a total pair energy for the configuration. Note that this pair energy is slightly different from that used in MD simulations, as the simulation potentials are at best site−site potentials. All energies are counterpoise-corrected.

In Table 4, the mole fraction, the number of the particular configuration, and the total interaction energies are listed, along with the pairwise-sum interaction energy.

The pair energies of $n_{DMSO} = 0.5$ are, of course, identical to the total interaction energy since only one pair of molecules composes the cluster.

For $n_{DMSO} = 0.33$, there are large deviations (13−16 kJ/mol) between the full interaction energy and the pair energy for the two most stable configurations. These configurations differ from the others in structure since they have rings with eight atoms involved. Interestingly, there are many configurations that exhibit no many-body effects at all. Considering only the pair energies, one finds that the energetic order of the configurations changes. In the case of MP2/RI, the pair treatment favors configuration 0.33-IV, where both water molecules are coordinated via the DMSO oxygen atom. For both cases, B3LYP and MP2/RI, there is no such big energy gap of 5 kJ/mol between the most stable and the next stable configuration for the pair energies as was the case for the total interaction energies.

Table 4. Pairwise Additivity of the Interaction Energies[a]

		B3LYP			MP2/RI		
n_{DMSO}	no.	IE	IE_{pair}	ΔIE	IE	IE_{pair}	ΔIE
0.5	I	−40.0	−40.0	0.0	−37.5	−37.5	0.0
	II	−33.9	−33.9	0.0	−32.3	−32.3	0.0
	III	−29.6	−29.6	0.0	−28.1	−28.1	0.0
	IV	−25.0	−25.0	0.0	−23.8	−23.8	0.0
	V	−20.4	−20.4	0.0	−21.0	−21.0	0.0
0.33	I	−84.3	−68.2	16.1	−77.2	−62.3	14.9
	II	−77.1	−64.0	13.1	−70.5	−58.4	12.1
	III	−68.1	−67.5	0.6	−64.4	−63.5	0.9
	IV	−67.8	−66.8	1.0	−65.7	−63.7	2.0
	V	−67.1	−66.5	0.6	−64.1	−63.2	0.9
	VI	−52.1	−51.3	0.8	−51.9	−51.0	0.9
0.25	I	−118.0	−99.0	19.0	−109.3	−91.5	17.8
	II	−117.9	−89.5	28.4	−107.9	−82.0	25.9
	III	−116.2	−96.0	20.2	−107.2	−87.8	19.5
	IV	−115.7	−102.4	13.3	−107.4	−94.5	12.9
	V	−114.4	−101.8	12.6	−106.7	−94.8	11.9
	VI	−109.1	−94.0	15.1	−100.4	−85.8	14.6
	VII	−99.8	−98.3	1.5	−96.0	−94.0	2.0
0.2	I	−162.2	−119.7	42.5	−149.5	−109.4	40.1
	II	−157.5	−129.5	28.0	−143.3	−118.3	25.0
	III	−157.0	−132.8	24.2	−144.8	−121.4	23.4
	IV	−156.9	−130.0	26.9	−145.0	−120.0	15.0
	V	−147.8	−122.9	24.9	−135.7	−112.6	23.1
	VI	−145.5	−127.3	18.2	−136.6	−119.6	17.0
	VII	−143.5	−124.2	19.0	−135.0	−115.8	19.2

[a] The total interaction energy obtained with B3LYP and MP2/RI is denoted as IE, and the pairwise-sum interaction energy is given in the IE_{Pair} columns. Their difference is ΔIE. All energies in kJ/mol.

At mole fraction $n_{DMSO} = 0.25$, there are larger many-body effects than at the higher mole fractions. The largest effect is observed for Rüssel configuration II. According to the pair energy, it is the most unfavorable configuration with a gap to the lowest-energy configuration of 13 kJ/mol. Similar results are observed for MP2/RI. Many-body effects are less pronounced for the methyl-group-free configurations.

The largest many-body effect is shown for the Rüssel configuration at mole fraction $n_{DMSO} = 0.2$ with 42.5 kJ/mol. This time the energetic order of the configurations is not disturbed by counting for pairs only, except for the Rüssel configuration, which is again the most unfavorable configuration with a gap to the lowest-energy configuration of 12 kJ/mol.

In summary, we find that at every mole fraction many-body effects are most pronounced in the Rüssel configuration. In comparison to the full cluster description, accounting only for pair interactions changes the picture significantly, particularly at mole fraction $n_{DMSO} = 0.25$. Our results show that many-body effects are very important, especially when methyl group contacts are participating.

7. Modeling Solvation

In our study of isolated clusters, we neglected solvation effects, which must be considered in order to take the first step toward an understanding of the condensed phase. Of course, we cannot treat this in the present work with a sufficient degree of sophistication as it would be too involved. However, to model solvation effects to a certain extent in our chosen framework, we (i) add water molecules and analyze the effect on structure and stability of the clusters and (ii) optimize cluster dimers to probe their stability. The latter approach in particular should reveal whether our small clusters can be identified in larger

Table 5. Stepwise Solvation by Adding One Water Molecule after the Other[a]

sequence 1	0.5-I	0.33-I	0.25-II	0.2-I
$r_{O(D)-H(W)}$	182.4	172.7	170.6	167.8
$a_{O...O-H}$	15.5	5.1	3.3	3.6
$r_{O(W)-H(D)}$	253.4	233.1	226.5	238.7
$a_{O...C-H}$	50.4	17.2	12.0	30.5
sequence 2	0.5-I	0.33-III	0.25-VII	
$r_{O(D)-H(W)}$	182.4	185.7	190.5	
$a_{O...O-H}$	15.5	17.3	18.0	
$r_{O(W)-H(D)}$	253.4	244.2	247.3	
$a_{O...C-H}$	50.4	32.5	32.8	
sequence 3		0.33-I	0.25-I	0.2-VI
$r_{O(D)-H(W)}$		172.7	195.2	192.2
$a_{O...O-H}$		5.1	18.1	14.1
$r_{O(W)-H(D)}$		233.1	229.4	227.0
$a_{O...C-H}$		17.2	16.6	15.6

[a] Distances r are given in picometers and angles a in degrees. The second and third row describe the distance and angle corresponding to the H1-type hydrogen bond. The last two rows correspond to the H3 contact.

aggregates. This would be appealing from the point of view of the classical paradigm that stable systems can be identified as entities in a supermolecule. For instance, we should be able to answer the question, whether our 1DMSO−2H_2O clusters can be found in larger clusters, e.g., 2DMSO−4H_2O.

We are well aware that the conclusions for "real" solvation from such an analysis must be drawn with great care and are affected by a certain degree of inherent speculation. Despite this speculative character, we shall explore the results from time-independent quantum chemical calculations to the fullest extent, which might finally guide findings from Car−Parrinello MD simulations.

7.1. Adding Water Molecules. A way to treat solvation is to add more and more solvent molecules and to track the changes. As we have calculated clusters of one DMSO molecule with up to four water molecules, it is possible to compare a sequence of clusters with an increasing amount of water, modeling solvation.

In Table 5, we list three sequences. Sequence 1 consists of all Rüssel configurations; in sequence 2, more and more water molecules are added to the DMSO oxygen atom (there is no possibility for a fourth water molecule), and in sequence 3, we added to the 0.33-Rüssel configuration water molecules at the DMSO oxygen atom. In the first row, the interaction energy per pair of the clusters is shown. The next two rows give the distance of the water hydrogen atoms to the DMSO oxygen atom and the corresponding O···O−H angle, reflecting the situation for a H1 hydrogen bond. The same is given for the smallest methyl−hydrogen−water−oxygen distance and the O···C−H angle in the last two rows, reflecting the situation for a H3 bond.

For the Rüssel sequence, the structural parameters in Table 5 clearly show that both bonds become more favorable upon solvation. The core structure, i.e., the 0.5-I basis structure, contracts and becomes more compact. We should recall optimal parameters for H1 and H3 contacts from section 4, which are 186.5 pm and 2.1° for H1 and 225 pm and 35.2° for H3. We see clearly that the core structure approaches these values upon solvation and improves on the H1 ideal values to produce even stronger hydrogen bonding. It is interesting to note that

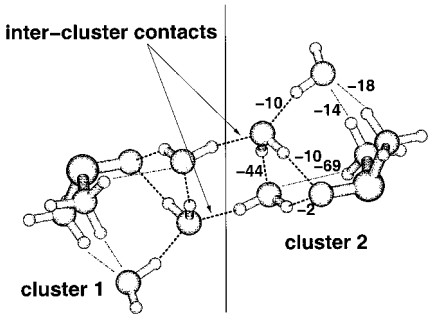

Figure 7. Optimized structure of two clusters. Numbers give deviations of distances from "bond" lengths in the isolated clusters in pm.

the trend has its optimum at 0.25-Rüssel and is a little reversed from the 0.25-Rüssel to the 0.2-Rüssel for three of the structure parameters.

The branching sequences 2 and 3 show two opposite trends: the H1 hydrogen bond becomes a little weaker upon solvation with a maximum at the 0.25 cluster for sequence 3, whereas the H3 becomes continuously stronger, again with a minimum at 0.25 for sequence 2. These trends are what one would expect, as we add here the water molecules to the oxygen atom, leading to a weakening of the existing hydrogen bond.

For all three sequences, the adding of water molecules leads to a reinforcement of the H3 contact.

7.2. Optimized Cluster Dimers. In condensed phases, the clusters would interact with each other. This interaction is mediated by the not yet saturated bonding sites of each cluster, leading to "intercluster" contacts. We studied several cluster dimers and found that the structure of each cluster is more compact in the dimer than in the isolated cluster; i.e., the hydrogen bond lengths are shortened, while the unsaturated contacts act as a glue (Figure 7 gives one typical example). Significantly, we observed that the spatial arrangement of a given configuration of the isolated supermolecule is seldom destroyed in the cluster dimer; i.e., there is typically no rearrangement of the *intra*cluster hydrogen bonds when compared to an isolated cluster or supermolecule with the corresponding cluster in a cluster dimer.

Particularly for the 0.25 clusters, we expect that a comparatively rigid, but nevertheless loosely and structurally highly diverse intercluster network evolves at low temperatures. This could prohibit the creation of a crystal-like ordered structure. We come to this conclusion because the spatially different 0.25 configurations are energetically similar, implying that all of them exist in condensed phase at the same time. Since they exhibit significant spatial differences and can thus not be easily transformed into one other through conformational changes, it becomes unlikely that this structurally highly diverse hydrogen bond network could experience gross rearrangements at low temperatures.

Furthermore, we conclude from the observation of energetically well-separated lowest-energy configurations at $n_{DMSO} = 0.5, 0.33, 0.2$ that the structure of the condensed phase at these mole fractions is probably governed by these lowest-energy configurations.

In accordance with the early assumptions in the literature,[1] two potential reasons for the freezing point depression emerge. One is the existence of stable *n*-hydrates of DMSO, which are connected with other lowest-energy clusters through intercluster

contacts. The other is the "glasslike" structure of the condensed phase at low temperatures, built up by stable clusters of different shapes.

For the relatively loose connection of the clusters, we find indications if we look at the number of unsaturated contacts left in the clusters. We find their contribution to be low (in percentage) for the possible configurations at $n_{DMSO} = 0.25$. A stronger argument for the "glasslike" structure is that these clusters are energetically in the same range, they are minimum configurations, but differ significantly in spatial arrangement.

8. General Discussion and Conclusion

Overall, the quantum chemical treatment of the clusters showed many structures deviating from what has previously been suggested in the literature (or what comes to mind when one thinks only in terms of Lewis formulas and partial charges). From the frequency analyses of all clusters, we conclude that the minimum structures described are dominated by the electronic structure, while the vibrations of the nuclei appear to have little effect on the interaction energies and thus the stabilization energies of the clusters. The agreement of the MP2/RI and the B3LYP results is very good. At almost every mole fraction, the Rüssel configuration was clearly the lowest-energy structure, with the exception of $n_{DMSO} = 0.25$.

The aim of this paper was twofold. The first aspect was to see what pure quantum chemistry could teach us in preparation for future MD simulations. In this study, the focus was on testing the quality of the intermolecular forces. We note that a combination of both "understanding intermolecular forces" and "treating the system dynamically" is necessary to provide final answers to a bulk problem of this kind. Second, we were interested in whether the unusual behavior at the mole fraction $n_{DMSO} = 0.25-0.33$ already emerges at the level of the intermolecular forces in small clusters. This would, for instance, lead to an explanation for the low melting points of this mixture at mole fractions of about $n_{DMSO} = 0.25-0.33$. A step toward finding a possible cause for the low melting point might be found by investigating small supermolecules.

As suggestions for MD simulations, we can give the following resumé. The minimum energy or optimized structures are certainly biased by the methyl groups of the DMSO. This is a secondary effect, but it is of the order of ~5 kJ/mol and thus not negligible. We demonstrated this in many different ways, e.g., with the electron localization function, with simple rotation curves, and with the shared-electron number method. We also tested the assumption of pairwise additivity and found a strong connection between methyl group favored structures and many-body effects. The many-body effects amount to 40 kJ/mol. In addition, we found many clusters at mole fraction $n_{DMSO} = 0.33$ that did not show any many-body effects. An example of this is the branching structure at the DMSO oxygen, and this kind of cluster is observed in MD simulations. Contrary to this, almost all the clusters at $n_{DMSO} = 0.25$ show many-body effects. The only exception is again the branching structure 0.25-VII, where all water molecules are coordinated via the oxygen atom, and indeed, this structure has also appeared in MD simulations,[4] although too briefly to be considered as a stable configuration. Thus, it appears to be conclusive that most MD simulations are not able to account for all other $1DMSO-3H_2O$ clusters, because pairwise additivity is assumed. It is not clear how important the minimum structures are for a condensed-phase study, as already mentioned. Nevertheless, our results suggest that thorough investigations of the effect of neglecting many-body effects and of using the united-atom ansatz in simulations could be enlightening. The first assumption could in principle be circumvented by the use of polarizable pair potentials, and the second could be circumvented by using an all-atom ansatz. Note that in the Car–Parrinello type of simulation both assumptions are avoided implicitly. This type of simulation is now in progress in our group.

For the explanation of the complicated phase diagram, respectively, of the low melting point, Havemeyer[2] referred to lattice theories. She claimed that "a structure could be formed of subunits of (two) water tightly bound to one DMSO molecule, with each such subunit more loosely bound to the next subunit. Hence, the over-all structure would be held together by bonds of varying strength or force." This mixture would consist of a variety of such configurations arranged in chains or groups. Because of the lack of regularities, no standard crystallization would be observed. In other words, at low temperatures, it becomes more and more unlikely that the hydrogen bond network undergoes gross rearrangements. Thus, a comparatively rigid and structurally highly diverse network evolves at low temperatures, prohibiting the generation of a crystal-like ordered structure. Particularly for the $1DMSO-3H_2O$ clusters, many different configurations lie in the same interaction energy range. Considering also the amount of unsaturated contacts, especially in configurations 0.25-I, 0.25-II, 0.25-III, and 0.25-IV, we see indications that the usual crystallization process cannot take place. For the $1DMSO-2H_2O$ clusters, some configurations (0.33-III, 0.33-IV, 0.33-V) also exhibit only few unsaturated contacts and lie in the same energy range. In opposition to the $1DMSO-3H_2O$ clusters (i) these are not the lowest minimum configurations and (ii) these configurations are easily interchangeable through simple rotation, leaving no reason for "glasslike" transitions.

We are currently performing CPMD simulations in extension of this work, which are intended to give further insight into the dynamics of these cluster interactions.

Acknowledgment. The authors thank Prof. B. A. Hess, Dr. A. J. Dyson, Prof. J. Hutter, Prof. H. Huber, Dr. D. J. (Bernardt) Searles, and D. Dath. B.K. would furthermore like to thank the DFG for financial support.

JA017703G